# Polarimetric studies of Comet C/2009 P1 (Garradd)

H. S.  $Das^{1\star}$ , B. J.  $Medhi^2$ , S.  $Wolf^3$ , G.  $Bertrang^3$ , P.  $Deb\ Roy^1$  and A.  $Chakraborty^1$  Department of Physics, Assam University, Silchar 788011, India.

- <sup>2</sup> Aryabhatta Research Institute of Observational Sciences, Manora Peak, Nainital 263129, India
- <sup>3</sup> Institut für Theoretische Physik und Astrophysik, Universität zu Kiel, Leibnizstr. 15, 24118 Kiel, Germany

Accepted 2013 September 26. Received 2013 September 23; in original form 2012 December 12

# ABSTRACT

the optical imaging polarimetric observations of comet C/2009 We present P1(Garradd) at three different phase angles e.g., 28.2°, 28.1° and 21.6°. The observations were carried out using IUCAA Faint Object Spectrograph and Camera mounted on Cassegrain focus of the 2-m Telescope of IGO, IUCAA, Pune in R<sub>comet</sub>, R photometric bands, on 21 and 22 March 2012 and ARIES Imaging Polarimeter mounted on Cassegrain focus of the 1.04-m Sampurnanand Telescope of ARIES, Nainital in R photometric band, on 23 May 2012. We show the presence of a jet activity in the rotational gradient treated image of comet Garradd at phase angle 28.1°. These jets are mainly oriented towards the Sun and extended up to  $\sim 5100$  km from the cometary photocenter. The antisolar extension of jet seems to be fainter, which is extended up to  $\sim 1800$  km. It is found that the comet Garradd shows negative polarization at phase angle 21.6°. The degree of polarization derived for Garradd is in good agreement with other comets at nearly similar phase angles e.g., comets 67P/Churyumov-Gerasimenko, 22P/Kopff, 1P/Halley, C/1990 K1 (Levy), 4P/Faye, and C/1995 O1 (Hale-Bopp) at phase angle  $\sim 28^{\circ}$ , and 47P/Ashbrook-Jackson at phase angle  $\sim 21.6^{\circ}$ , respectively. It is also found that the degree of polarization of dusty coma of comet Garradd at phase angle  $\sim 28^{\circ}$  is high but, not as high as in the case of comet Hale-Bopp.

**Key words:** polarization – scattering – comets: general – dust, extinction.

# INTRODUCTION

The comet C/2009 P1(Garradd) was named after the Australian astronomer Gordon J. Garradd from Siding Spring Observatory, Australia, who discovered the comet on four images obtained between August 13.77 and August 13.81 2009, at a heliocentric distance of 8.7 AU. In the same year 2009, B. G. Marsden also calculated the parabolic orbit of the comet Garradd. The aphelion distance of the Garradd is  $\sim 5000 - 5500$  AU, which was estimated by Nakano in the year 2011 (Nakano 2011). It is to be noted that the location of inner Oort cloud is somewhere in between 2,000 and 20,000 AU. So, the comet Garradd may belong to the inner Oort cloud family, but it is difficult to comment whether or not comet Garradd is dynamically new. The comet reached its perihelion on December 23, 2011 (r = 1.55 AU) and its closest approach to the Earth was on March 5, 2012 ( $\triangle =$ 1.27 AU). The visual magnitudes of comet Garradd were 9.7 and 12.4 on March 21 and May 23, 2012 respectively, which was sufficiently bright enough for observation in optical domain.

\* E-mail: hsdas@iucaa.ernet.in (HSD)

The apparition of the comet Garradd provided us a very good opportunity to conduct different studies using photometric, spectroscopic and polarimetric techniques to understand the physical properties of cometary dust grains (Bodewits et al 2012, DiSanti et al. 2012, Hadamcik et al. 2012, Kiselev et al 2012, Tanigawa et al. 2012 and Villanueva et al. 2012). The preliminary results obtained by the different investigators show high production of dust in the comet Garradd, far away from the Sun. All observations indicated that it belongs to a dusty comet family. According to Swift's Ultra-Violet and Optical Telescope's (UVOT) data, at comparable heliocentric distances the comet Garradd's behavior is very similar to the comet Hale-Bopp (Bodewits et al. 2012).

The polarimetric study of comet over various scattering angles and wavelengths could provide very useful information about the nature of cometary dust such as composition, albedo, size distribution of grains etc. (Kikuchi et al. 1987; Chernova et al. 1993; Ganesh et al. 1998; Das et al. 2004, 2008a, 2008b, 2010, 2011; Das & Sen 2006, 2011; Hadamcik et al. 2007, 2010). In this paper, we present the results of optical polarimetric study of the comet Garradd at three different scattering angles. The rest of the paper is organized

as follows. In Section 2 we present the observations and data reduction. Our results are presented in section 3. Finally, a discussion is presented in Section 4, and we conclude with a summary in Section 5.

# OBSERVATIONS AND DATA REDUCTION

The polarimetric observations of the comet Garradd were carried out at two different telescopes in India; (1) 2-m Telescope of Girawali Observatory at Inter University Center for Astronomy and Astrophysics (IUCAA), Pune (IGO, Latitude:  $19^{\circ}5'$  N, Longitude:  $+73^{\circ}40'$  E, Altitude = 1000 m), and (2) 104-cm Sampurnanand Telescope of Aryabhatta Research Institute of observational sciencES (ARIES), Nainital (AST, Latitude: 29°22′ N, Longitude: 79°27′ E, Altitude = 1951 m).

#### 2.12-m Telescope, Girawali Observatory, IUCAA

The 2-m telescope of IGO has a Cassegrain focus with a focal ratio of f/10. The IUCAA Faint Object Spectrograph and Camera (IFOSC) was using as a focal plane instrument for the polarimetric observation. The imaging was done on March 21 and 22, 2012 using an EEV 2K × 2K pixels thinned, back-illuminated CCD which provides an effective field of view of  $10.5' \times 10.5'$  and each pixel corresponds to 0.3 arcsec on the sky. The gain and read out noise of the CCD are 1.5 e<sup>-</sup>/ADU and 4 e<sup>-</sup>, respectively. IFOSC's capabilities are enhanced with an imaging polarimetric mode with a reduced circular field of view of about 2 radius. It makes use of a Wollaston prism and a half-wave plate (HWP) in between camera lens and field lens, which covers the wavelength ranges from 350 to 850 nm. The rotatable HWP gives components of the electric vector polarized orthogonally of varying intensities after emerging out of the Wollaston prism. The axis of Wollaston prism is aligned to the north-south (NS) axis of the telescope, and the HWP is placed in such a way that its fast axis aligned to the axis of the Wollaston prism. Two successive positions of the HWP are needed to obtain the degree of polarization and the position angle of the polarization vector. The optical principle and design of present IUCAA polarimeter are given by Scarrott et al. (1983) and Sen & Tandon (1994). More details on the principles of the instrument are described in Ramaprakash et al. (1998) and Paul et al. (2012).

At a particular angle  $\beta$  of the HWP, the intensities of the two orthogonally polarized beams are measured. When the HWP rotates an angle  $\beta$ , the electric vector rotates through an angle  $2\beta$ . A ratio  $R(\beta)$  is defined by;

$$R(\beta) = \frac{I_e/I_o - 1}{I_e/I_o + 1} = p \cos(2\theta - 4\beta)$$
 (1)

where  $I_e$  and  $I_o$  are extraordinary and ordinary image, p is the fraction of the total light in the linearly polarized condition,  $\theta$  is the position angle of the plane of polarization and  $\beta$  is the angle of HWP. When the HWP rotates successively  $22.5^{\circ}$ ,  $45^{\circ}$  and  $67.5^{\circ}$  from an initial position  $0^{\circ}$ , the position angles of the polarized components respectively rotate  $45^{\circ}$ ,  $90^{\circ}$  and  $135^{\circ}$  from the initial position. The linear polarization and position angle values could be calculated from the normalized Stoke's vectors q = Q/I, u = U/I,  $q_1 = U/I$ 

 $Q_1/I$ ) and  $u_1$  (=  $U_1/I$ ) when the value of  $\beta$  is  $0^{\circ}$ ,  $22.5^{\circ}$ ,  $45^{\circ}$ and  $67.5^{\circ}$ , respectively.

The linear polarization (p) and position angle  $(\theta)$  of the polarization vector is defined by:

$$p = \sqrt{(q^2 + u^2)}$$
 and  $\theta = 0.5 \tan^{-1}(q/u)$  (2)

In principle p and  $\theta$  can be determined by using only two Stoke's vectors q and u. But, the additional two values  $(q_1 \text{ and } u_1)$  are measured at  $\beta = 45^{\circ}$  and  $67.5^{\circ}$  due to nonresponsivity of the system (Ramaprakash et al. 1998).

Both the narrow-band filter ( $R_{comet}$ ,  $\lambda = 0.684 \ \mu m$ ,  $\Delta \lambda = 0.009 \ \mu m$ ) and broadband filter (R,  $\lambda = 0.630 \ \mu m$ ,  $\Delta \lambda = 0.120 \ \mu m$ ) were used for polarimetric observations. These filters reduce the contamination by gaseous species present in the comet.

#### 2.2 104-cm Sampurnanand Telescope, ARIES

The 1.04-m Sampurnanand Telescope of ARIES has a Cassegrain focus with a focal ratio of f/13. ARIES Imaging Polarimeter (AIMPOL) was using as a back-end instrument for polarimetric observation, which consists of a halfwave plate (HWP) modulator and a beam-splitting Wollaston prism analyzer. The data were obtained on May 23, 2012 using TK 1024×1024 pixels CCD camera mounted on the Cassegrain focus of AST. The observations were carried out in R filter ( $\lambda = 0.630 \ \mu m, \ \Delta \lambda = 0.120 \ \mu m$ ). Each pixel of the CCD corresponds to 1.73 arcsec and the field-of-view is  $\sim 8$  arcmin diameter on the sky. The gain and read out noise of the CCD are 11.98 e<sup>-</sup>/ADU and 7.0 e<sup>-</sup>, respectively. The working principle and design of AIMPOL are almost similar to IUCAA's imaging polarimeter. The detail about AIMPOL and data reduction procedures are available in Rautela et al. (2004), Medhi et al. (2008, 2010) and Pandey et al. (2009).

#### 2.3Observational procedure

The geometrical conditions during the time of observation are shown in the Table 1, which are collected from JPL's HORIZONS system of NASA. The standard stars for null polarization and zero-point of the polarization position angle were taken from Schmidt et al. (1992), Turnshek et al. (1990) and HPOL ( http://www.sal.wisc.edu/HPOL/tgts/HD251204.html ), respectively. The results of polarized and unpolarized standard stars in R filter and their corresponding values from the above cited literatures are depicted in the Table 2. The degree of polarization (p) and position angle  $(\theta)$  with their corresponding errors from the literatures are given in the fourth and fifth column, while the observed value of polarization  $(p_{obs})$  and position angle  $(\theta_{obs})$  with their corresponding errors are presented in the sixth and seventh column of the Table 2. The position angle of the unpolarized stars HD94851 and HD154891 are not available in the literature and the polarization value for HD154891 is available only for B photometric band. Since the zero position of HWP is not systematically aligned with the north-south direction or with sun-ward direction, the offset angle has estimated using  $\theta_0 = (\theta - \theta_{obs})$  and given in eighth column of the Table

**Table 1.** Log of the observations. Observatory, UT date, heliocentric distance (r), geocentric distance ( $\triangle$ ), apparent total visual magnitude  $(m_v)$ , phase angle ( $\alpha$ ), position angle of extended Sun – comet radius vector ( $\phi$ ), projected diameter for 1 pixel (D), filters and exposure time (time for one exposure × number of exposures used for the results) during the observations.

Observatory	UT date	r (AU)	$\triangle$ (AU)	$m_v$	α (°)	φ (°)	$\begin{array}{c} D \\ (\mathrm{km} \ \mathrm{px}^{-1}) \end{array}$	Filters	Exposure time
IGO, Pune (2 m)	March 21, 2012	1.96	1.36	9.71	28.2	157.7	304	$R_{comet}$ R	$720s \times 1$ $180s \times 1$
IGO, Pune (2 m) AST, Nainital (1.04 m)	March 22, 2012 May 23, 2012	1.97 $2.52$	$\frac{1.38}{2.75}$	9.75 $12.41$	$28.1 \\ 21.6$	153.9 $101.1$	$307 \\ 3440$	R R	$60s \times 1, 30s \times 3$ $100s \times 10$

**Table 2.** Results of standard polarized and unpolarized stars at R-filter. p and  $\theta$  from literature (Schmidt et al. 1992; Turnshek et al. 1990 and HPOL).  $p_{obs}$  and  $\theta_{obs}$  from observations. Offset angle is calculated using the relation:  $\theta_0 = (\theta - \theta_{obs})$ .

Observatory	UT date	Star	p (%)	θ (°)	$p_{obs}(\%)$	$\theta_{obs}$ (°)	$\theta_0$
IGO	March 21, 2012	HD251204 GD319	$5.33\pm0.05$ $0.09\pm0.09$	153.7 140.0	$5.30\pm0.24$ $0.37\pm0.29$	$155.8 \pm 1.3$ $138.6 \pm 22.4$	-2.1° 1.4°
	March 22, 2012	HD251204 HD94851	$5.33 \pm 0.05$ $0.06 \pm 0.02$	153.7 NA	$5.30\pm0.23$ $0.21\pm0.09$	$155.7 \pm 1.24 \\ 148.3 \pm 12.5$	−2.0° −
AST	May 23, 2012	HD154445 HD155197 HD154892	3.96±0.07 4.31±0.04 0.05±0.03	99.25 111.59 NA	$3.68\pm0.07$ $4.27\pm0.03$ $0.07\pm0.05$	$88.91\pm0.56$ $102.88\pm0.18$ $22\pm20$	10.34° 8.71° –

By definition the degree of linear polarization can be either positive or negative but the value of polarization p obtained from the equation (2) is always positive. Actually the sign of polarization depends on the position angle of the polarization plane with respect to the scattering plane in the equatorial reference system. The values  $P_r$  and  $\theta_r$  for the scattering plane could connect with the quantities  $P_{obs}$  and  $\theta_{obs}$  using the following relation (Chernova et al. 1993);

$$P_r = P_{obs}.cos2\theta_r, \quad \theta_r = \theta_{obs} - (\phi \pm 90^\circ),$$
 (3)

where  $\phi$  is the position angle of the scattering plane and the sign in the bracket is chosen to ensure the condition  $0 \leqslant \phi \pm 90^{\circ} \leqslant 180^{\circ}$ . If  $\theta_r$  is either  $0^{\circ}$  or  $90^{\circ}$ , the linear polarization will be either close to the scattering plane or perpendicular to it. For AST observation, the average value of  $\theta_r$  is estimated to be 129.8°. Therefore the polarization values will be negative in this case, which is quite expected at  $\alpha = 21.6^{\circ}$ .

We have used different astronomical image processing softwares e.g., IRAF, IRIS and FITS Viewer to analyze the observed images. Each image is corrected for bias and flat. The photometric center was found with a precision of 0.1 pixels by fitting the inner part with a Gaussian profile. The two perpendicularly polarized images ( $I_e$  and  $I_o$ ) obtained in a single plate (for a particular rotation angle of the HWP) are then trimmed with same dimension (IGO:  $176 \times 176$  pixels and AST:  $41 \times 41$  pixels). Thus, a total of eight images having the same dimension are obtained for  $0^{\circ}$ ,  $22.5^{\circ}$ ,  $45^{\circ}$  and  $67.5^{\circ}$  rotation of the HWP for one set of observation. Since the comet is faint, the signal-to-noise ratio is increased through building each polarized components by adding the images for each orientation of the HWP. In one series of observation at R-filter from IGO on March 21, 2012 the stellar

trails are visible in the inner coma region after the images have been centered and added. So, we have not considered those images for our analysis.

The intensity images are obtained by adding two polarized components. The total intensity is given by; I = $(I_e + I_o)_{0^{\circ}} = (I_e + I_o)_{22.5^{\circ}} = (I_e + I_o)_{45^{\circ}} = (I_e + I_o)_{67.5^{\circ}}.$ The sky background is estimated using standard task in IRAF/IRIS and the average value of background is subtracted from the scientific image. The method of sky subtraction depends on the object and sky condition at the time of observation. Background subtraction is a very difficult task for comets because the dusty coma may extends up to the infinity. Usually the sky background is measured in several positions at the edge of the images, as far as possible, which is about 35000km for IGO and 70000km for AST respectively, from the photometric center of the comet, keeping in mind that there could be still some signal of the coma. The sky background is carefully estimated and subtracted for both the cycle of observations and normalize by transform the images in e<sup>-</sup>/s. After normalization, the intensity image is treated by the rotational gradient technique to detect the image structures. The image emphasizes the high gradient regions in brightness (Hadamcik et al. 2003a; Hadamcik et al. 2010). The rotational gradient creates two images, one with a radial shift (in pixel) and the other with a rotational shift (in degree). The two images are added to create the final image. This method is useful for enhancing the low contrast structures that are radially organized about some points in an image. To study the high gradient regions on the intensity images (i.e., to find jet features) treated intensity images have been built using Larson-Sekanina's rotational gradient technique (Larson and Sekanina 1984). Finally, the polarization maps have been built up using the images of four polarized components.

# 3 RESULTS

### 3.1 Intensity images

# 3.1.1 Radial intensity profiles

A radial profile in intensity could help to detect the deviation from an isotropic coma. To study the properties of coma the radial surface brightness profile is measured, because it is easy to extract the slopes. The intensity of coma could be described by using a power law;  $I = k.r^q$  where k is the scaling factor for the coma, r is the distance from the photocenter and q is the slope. When q = -1, it is called canonical slope (Jewitt & Meech 1987; Goidet-Devel et al. 1997; Lamy et al. 2009). The canonical coma model of a nucleus produces a steady-state dust outflow that exhibits a constant slope of -1. Actually differences from this value of slope indicate the variations from the standard model, which generally caused by the temporal changes in dust production, radiation pressure and change in the physical properties of the grains e.g., sublimation, fragmentation, changes in optical properties etc. The variations of intensity versus photocentric distance in log scale is plotted in Fig. 1(a) and 1(b) for both IGO and AST observations. During the entire observation it is noticed that the intensity decreases with the increasing distance from photocenter. At a small distance from the photocenter the profiles are dominated by the atmospheric seeing. The seeing radius  $(r_s)$  for IGO and AST observations were found as 2 arcsec and 4 arcsec, respectively. The radial profile is canonical in nature with a slope of -1 in log scale when the distance to the photocenter is, (i) in between 2000 km to 25000 km on March 22, 2012 and (ii) in between 8000 km to 30000 km on May 23, 2012. It is to be noted that the canonical slope can be adjusted by the subtraction of sky background, if necessary. If the comet is faint, then sometimes the signal at the outer region of the coma may lesser than the sky background, so care should be taken to subtract the sky background.

# 3.1.2 Profiles through the intensity images

The variation of intensity inside coma is analyzed by the radial cuts through the intensity images. The decrease in intensity with a gradual increase in distance from the photocenter is being well noticed in both the solar and antisolar direction (Fig. 1a & 1b). The intensity is high in the solar direction as compare to antisolar direction. The changes of slope for decrease in intensity as a function of the photocenter distance in log scale is being compared for both the March and the May observations. It is found that the slope is dominated by the seeing near the photocenter if the distance is less than 2000 km in IGO observation and less than 8000 km in AST observation. The slope of the intensity increases gradually with distances from photocenter in the solar direction whereas slope is found to be decreasing in the antisolar direction for both the cycle of observations. Our results are in good agreement with Hadamcik et al. (2013). In March observations, the intensity falls with an average slope of -1 in the antisolar direction and -1.2 in the solar

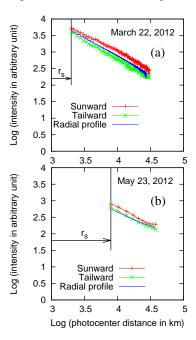


Figure 1. Cuts through the coma sun-ward, tail-ward and radial profile for the two periods of observations. Vertical lines represent the seeing radius  $(r_s)$  limits for each period.

direction when the distance is in between 2000 km to 30000 km from the photocenter. But, in the May observations, the average slopes are found to be -0.95 when the distance is in between 8000 km to 30000 km in the antisolar direction and of about -1.1 for the same range of distances in the solar direction.

# 3.1.3 Coma morphology

The intensity image with contours and their corresponding treated intensity image using rotational gradient method are shown in Fig. 2a and 2c, for IGO observation. The position angle (PA) of the extended Sun and comet radius vector is 153.9°. In the treated image, a strong dust jet feature seems to be present in the solar direction with an extension of  $\sim 5100~\rm km$  from the photocenter. The PA of the jet is about 311°. The tail-ward extension of the jet is  $\sim 1800~\rm km$  and seems to be fainter.

Fig. 2b and 2d present the intensity image with contours and their corresponding treated image using rotational gradient method for AST observation. The position angle (PA) of the extended Sun and comet radius vector is 101.1°. The coma is extended slightly in tail-ward direction and the dust jet feature seems to be absent on May 23, 2012.

# 3.2 Linear polarization

#### 3.2.1 Aperture Polarization

To study the evolution of whole-coma polarization, the polarization values are determined from the integrated flux obtained through all the polarized components for increasing apertures. As discussed earlier, the two perpendicularly polarized images obtained in a single image are trimmed to the same dimension. Thus, a total of eight images having the

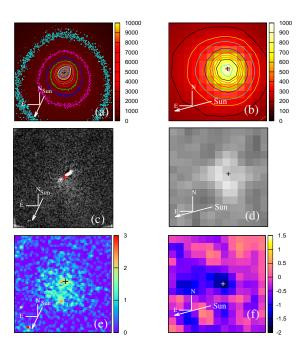


Figure 2. (a) and (b): Intensity image with contours (the levels are in ADU) for IGO and AST; (c) and (d): The rotational gradient treated image are shown for comet C/2009 P1 Garradd for IGO and AST and (e) and (f): Polarization map (the levels are in %) for IGO and AST at phase angles  $28.1^{\circ}$  and  $21.6^{\circ}$  respectively. The field of view for all the figures is  $45000 \text{ km} \times 45000 \text{ km}$ . The '+' mark denotes the optical center of the comet. The position angles (PA) of extended Sun – Comet radius vector for IGO and AST are  $153.9^{\circ}$  and  $101.1^{\circ}$  respectively.

same dimension are obtained for the four different positions of the HWP. The eight images are properly aligned , and the magnitude and their corresponding error at different apertures are computed. The degree of linear polarization and position angle are then calculated using a FORTRAN program based on equations (1) and (2).

We have only four sets of exposures in R-filter on 22 March 2012. Since the comet is faint, the signal-to-noise ratio is enhanced through building each polarized components by adding the images for each orientation of the HWP. Thus the 16 images are trimmed to obtained 16 extraordinary and 16 ordinary images. Finally these images are properly aligned and combined to build eight perpendicularly polarized images. For the AST observation, 40 images are used to calculate the average polarization value. The polarization  $(p_{obs})$  and the position angle  $(\theta_{obs})$  obtained through different apertures at both the IGO and AST observations are given in the Table 3. The variation of polarization in different apertures is small for both the narrow-band and broad-band filters. It is also found that on 21 and 22 March observations, at phase angle  $\sim 28^{\circ}$  the degree of polarization is almost similar for  $R_{comet}$  and R filter. This confirms that the gaseous contamination by the emission lines through broadband filter is negligible. For IGO observations, the polarization values obtained from this work are in good agreement with Hadamcik et al. (2013).

The polarization values obtained during the observation on May 23 show the negative polarization value at phase an-

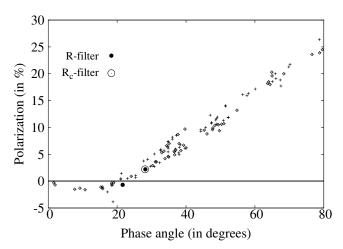


Figure 3. Polarization vs phase angle plot for different dusty comets at  $R_{comet}$ -filter (denoted by '+' symbol) and R-filter (denoted by 'o' symbol). The symbols '•' and 'o' represent observed polarization value for comet C/2009 P1 Garradd at R-filter and  $R_{comet}$ -filter respectively. The linear polarization data of different comets are taken from Database of Comet Polarimetry by Kiselev et al. (2006).

gle  $21.6^{\circ}$  as expected (already discussed in Section-2.3). In the Fig. 3, the polarization values obtained from the present observation at  $\lambda = 0.684 \mu m$  and  $0.630~\mu m$  are shown along with the polarization values of other comets taken from Kiselev et al. (2006).

# 3.2.2 Polarization maps

The polarization maps are created using the four properly aligned polarized components of the object. We built the polarization maps for March 22 and May 23 observations at R-filter. It is to be noted that the polarization map is obtained using a CL script written in IRAF and the map is shown in Figure 2e and 2f for IGO and AST observations, respectively. The polarization maps for both the cycle of observations are found to be in good agreement with the aperture polarization values. In March observations the degree of polarization is  $\sim 3\%$  at  $\alpha = 28^{\circ}$  when the aperture fits close to photocenter. But, at a distance of  $\sim 4000$  km from the photocenter the degree of polarization varies from 3% to 2%, however it is found quite uniform within  $\sim 10000 \text{ km}$ from the photocenter in both solar and tail-ward direction. In the outer coma the degree of polarization varies in between 2\% and 0.5\%. In the month of May, both the positive and negative polarization are observed in the polarization map throughout the coma at  $\alpha=21.6^{\circ}.$  The degree of polarization close to the photocenter is about -1.6% and in the inner coma varies between -1.8% and -0.2%. The positive polarization is mainly noticed in the outer coma and varies between 0.04 and 1.4%. The variations of degree of polarization in the inner and outer coma suggests that the physical properties of cometary dust varies with the distance from the photocenter.

	-		
1		`	

Diameter (in km) UT Date	$\overset{\rightarrow}{\operatorname{Filter}}$	4000	8000	16000	20000	24000	30000	$\theta_{obs}$ (in degrees)
March 21, 2012	$R_{comet}$	$2.2 {\pm} 0.3$	$1.9 \pm 0.2$	$1.9 \pm 0.2$	$2.0 \pm 0.2$	$2.0 \pm 0.3$	$2.0 \pm 0.4$	$154.1 \pm 4.0$
March 22, 2012	R	$2.0 \pm 0.1$	$2.2 {\pm} 0.1$	$2.3 \pm 0.1$	$2.4 \pm 0.1$	$2.6 \pm 0.1$	$2.9 \pm 0.2$	$154.6 \pm 1.4$
May 23, 2012	R	-	-	$-0.99 \pm 0.7$	$-0.68{\pm}0.8$	$-0.95{\pm}0.6$	$-0.87{\pm}0.6$	$140.8 \pm 9.4$

**Table 3.** Linear Polarization and the position angle  $(\theta_{obs})$  of polarization vector for comet Garradd at different apertures and wavelengths.

# DISCUSSION

Levasseur-Regourd et al. (1996) studied a polarimetric database of 22 comets and from the nature of the phase angle dependency concluded that broadly there are two class of comets exist. But, later on Hadamcik & Levasseur-Regourd (2003b) suggested that comet Hale-Bopp itself represents an another separate class of comet, marked by unusual high polarization. This classification is prominent only when the phase angles are higher than 35°. At phase angles between 80 to 100°, the degree of polarization tends to be higher than 20% for a group of comets which is known as Dust rich comets and smaller than 15% for another group which is known as Gas rich comets. The observed linear polarization values of the comet Garradd at  $\alpha = 28^{\circ}$  and  $21.6^{\circ}$  are compared with other comets observed by different investigators at similar phase angle (Chernova et al. 1993, Gural'Chuk et al. 1987, Kiselev et al. 2006, Le Borgne et al. 1987, Myers 1985, Manset & Bastein 2000, Renard et al. 1996). We found that the comets 67P/Churyumov-Gerasimenko, 22P/Kopff, 1P/Halley, C/1990 K1 (Levy), 4P/Faye, and C/1995 O1 (Hale-Bopp) were observed at phase angle close to 28° and the comet 47P/Ashbrook-Jackson at 21.6°, and our results are almost comparable with the results obtained for dusty comets. The degree of linear polarization of the dusty coma shows a high degree of linear polarization at phase angle 28°, but not exceptionally high as that of comet Hale-Bopp. Kiselev et al. (2012) also made a polarimetric observation of the comet Garradd at different phase angles. The degree of polarization obtained from our data at  $\alpha = 21.6^{\circ}$  and  $28^{\circ}$ are in good agreement with their results at  $\alpha = 22^{\circ}$  and 30°, respectively. They also found that the polarization of comet Garradd measured in larger areas of coma is almost comparable with the data available for most of the dusty comets.

The active comets having well shaped jets show higher polarization than less active comets (Hadamcik et al. 2003a). Jets are usually composed of very small sub-micron size particles or large fluffy aggregates. The comets which have higher value of maximum polarization  $(P_{max})$  show wellstructured silicate features in the 10  $\mu m$  wavelength domain (Levasseur-Regourd et al. 1996). This suggests the presence of sub-micron size particles or constituent grains in high porous aggregates. The albedo of these particles is relatively high (Hanner 1999). The study of comet Hale-Bopp revealed the existence of a highly porous dust aggregates in the jets coming out from the nucleus (Hayward et al. 2000, Hadamcik & Levasseur-Regourd 2003b), which are also observed in the laboratory experiment (Hadamcik et al. 2002) and in the ground based observation of comet C/1999 S4 (LINEAR) (Hadamcik & Levasseur-Regourd 2003c). In our

observations of comet Garradd a sun-ward jet is observed which extends up to 5100 km in the month of March and also noticed in the polarization map.

Hadamcik et al. (2012, 2013) has observed the comet Garradd applying imaging polarimetric technique and found that the polarization value appear to be almost constant for the small apertures inside the coma, including the tail-ward fan. Both the ground-based observations and space-based observations of comet Garradd have shown a high production of dust far away from the Sun (Villanueva et al. 2012; Bodewits et al. 2012). Bodewits et al. (2012) reported Swift's UV-Optical telescope (UVOT) observations of comet Garradd at regular intervals at heliocentric distances between 3.5 and 1.7 AU on its inbound trajectory. From the UVOT grism spectra of the comet Garradd they found that its behavior is nearly similar to the behavior of comet Hale-Bopp at comparable heliocentric distances. The polarization value obtained from our observation at  $\alpha = 28^{\circ}$  is about 2% for  $\lambda = 0.684 \ \mu m$ , but at such phase angle and wavelength the polarization value for the comet Hale-Bopp is  $\sim 4\%$  (Manset & Bastien 2000). It is clear from our analysis that the comet Garradd does not show any resemblance with comet Hale-Bopp at such phase angle. This contradicts the result with Bodewits et al. (2012).

To study the linear polarization properties at small phase angles, Hadamcik & Levasseur-Regourd (2003a) built the polarization maps for comets 1P/Wild 2, C/1995 O1 (Hale-Bopp), C/1990 K1 (Levy), 47P/Ashbrook-Jackson and 22P/Kopff. In case of comet 22P/Kopff, it is found that at  $\alpha = 18^{\circ}$  the inner coma produced a strong negative polarization of -6% surrounding the photocenter with an extension of about 1500 km. The polarization map of comet Hale-Bopp at  $\alpha = 19.6^{\circ}$  shows a negative polarization of  $(-2\pm 1)\%$  as compared to the whole coma polarization of  $(1.5 \pm 0.5)\%$ . The negative polarization is also observed in comets C/Levy and 47P/Ashbrook-Jackson near the inversion angle i.e., at  $\alpha = 17.6^{\circ}$  and  $21.3^{\circ}$ . Kiselev et al. (2012) also observed the negative polarization for the comet Garradd at phase angle 22° and 13°. They got a minimum value of about -2% near  $\alpha = 13^{\circ}$ . Like all those, the negative polarization has also been observed for the comet Garradd at  $\alpha = 21.6^{\circ}$  in our May observation. The polarization map obtained at  $\alpha = 21.6^{\circ}$  is shown in the Fig. 2f. The innermost coma produces negative polarization of  $\sim -1.6\%$ , which is called as circumnucleus halo, surrounding a radius of about 10000 km from the photocenter. The positive polarization varies between 0.04 and 1.4 %, which is mainly noticed in the outer coma. The variation of both positive and negative polarization in all possible direction of coma signifies the variation in the physical properties of dust in the comet.

# 5 SUMMARY

- (a) Comet C/2009 P1 (Garradd) has been observed for three nights in the month of March and May 2012 in polarimetric mode at the phase angles  $28.2^{\circ},\,28.1^{\circ}$  and  $21.6^{\circ}.$  A small value of  $\sim-0.9\%$  polarization has been observed at phase angle  $21.6^{\circ}.$
- (b) The radial intensity profile of the comet is canonical in nature with a slope of -1 in log scale when the distance to the photocenter is (i) in between 2000 km to 25000 km on March 22, 2012 and (ii) in between 8000 km to 30000 km on May 23, 2013. The canonical coma produces a steady-state dust outflow. The decrease in intensity with a gradual increase in the photocentric distance is noticed in both the solar and antisolar direction of the comet. On March 22, 2012 the intensity falls with an average slope of -1 in the antisolar direction and -1.2 in the solar direction when the distance is in between 2000 km to 30000 km from the photocenter of the comet. On May 23, the average slopes are found to be -0.95 when the distance is in the range 8000 km to 30000 km in the antisolar direction and of about -1.1 for the same range of distances in the solar direction.
- (c) The degree of linear polarization of the dusty coma of the comet Garradd obtained from our observations at R and  $R_{comet}$  filters are in good agreement with the results reported by other investigators in similar phase angles. The dusty coma shows a high degree of linear polarization at phase angle  $28^{\circ}$ , but not as high as the comet Hale-Bopp.
- (d) Jet activity is observed in the treated intensity image of the comet Garradd in the month of March 2012, which seems to be absent in the May 2012 observation. These jets seem to be present in the solar direction with an extension of  $\sim 5100~\rm km$  in the projection on the sky. The position angle of the jet is about 311°. The antisolar extension of jet is  $\sim 1800~\rm km$  and seems to be fainter.

# 6 ACKNOWLEDGEMENTS

We are highly grateful to anonymous referee for their valuable suggestions and comments which definitely helped to improve the quality of the paper. We also acknowledge Jeremy R. Walsh of European Southern Observatory, Garching, Germany for useful discussion. We gratefully acknowledge IUCAA, Pune and ARIES, Nainital for making telescope time available. This work is supported by the Department of Science & Technology (DST), Government of India, under SERC-Fast Track scheme (FTP/PS-092/2011).

#### REFERENCES

- Bodewits D., Farnham T.L., AHearn M.F., Landsman W.B., 2012. Proceedings of the Asteroids, Comets, Meteors conference 2012. LPI contribution 1667, id.6084.
- Chernova G. P., Kiselev N. N., Jockers K., 1993, Icarus,  $103,\,144$
- Das H. S., Sen A. K., Kaul C. L., 2004, A&A, 423, 373
- Das H. S., Sen A. K., 2006, A&A, 459, 271
- Das H. S., Das S. R., Paul T., Suklabaidya A., Sen A. K., 2008a, MNRAS, 389, 787
- Das H. S., Das S. R., Sen. A. K., 2008b, MNRAS, 390, 1195.

- Das H. S., Suklabaidya A., Majumder S. D. and Sen A. K., 2010, Res. Astr. & Astroph., 10, 355
- Das H. S., Sen A. K., 2011, JQSRT, 112, 1833
- Das H. S., Paul D., Suklabaidya A. and Sen A. K., 2011, MNRAS, 416, 94
- DiSanti M. A., Bonev B. P., Villanueva G. L., Paganini L., Mumma M. J., Charnley S. B., Keane J. V., Meech K. J., Blake G. A., Bohnhardt H., Lippi M., 2012, Proceedings of the Asteroids, Comets, Meteors conference 2012. LPI contribution 1667, id.6407.
- Ganesh S., Joshi U. C., Baliyan K. S., Deshpande M. R., 1998, A&AS, 129, 489.
- Goidet-Devel B., Clairemidi J., Rousselot P., Moreels G., 1997, Icarus, 126, 78
- Gural'Chuk A. L., Kiselev N. N., Morozhenko, A. V., 1987, Kinematika Fiz. Nebesn. Tel, Tom 3, No. 3, p. 93 - 94
- Hadamcik E., Renard J.-B., Worms J.C., Levasseur-Regourd A.C., Masson M., 2002. Icarus 155, 497.
- Hadamcik E., Levasseur-Regourd A. C., 2003a. JQSRT, 79, 661.
- Hadamcik E., Levasseur-Regourd A. C., 2003b. A&A, 403, 757.
- Hadamcik E., Levasseur-Regourd A. C., 2003c. Icarus 166, 188.
- Hadamcik E., Levasseur-Regourd A.C., Leroi V. and Bardin D., 2007, Icarus 191, 459.
- Hadamcik E., Sen A. K., Levasseur-Regourd A.C., Gupta R. and Lasue J., 2010, A&A 517, A86
- Hadamcik E., Sen A. K., Levasseur-Regourd A. C., Gupta R., Lasue J., Botet R., 2012, Proceedings of the Asteroids, Comets, Meteors conference 2012. LPI contribution 1667, id.6200.
- Hadamcik E., Sen A. K., Levasseur-Regourd A. C., Roy Choudhury S., Lasue J., Gupta R., Botet R., 2013, MAPS, doi: 10.1111/maps.12114.
- Hanner M. S., 1999, Space Science Rev., 90, 99.
- Hayward T.L., Hanner M.S., Sekanina Z., 2000. ApJ, 538, 428.
- Jewitt D. C., Meech K. J., 1987, ApJ, 317, 992.
- Kikuchi S., Mikami Y., Mukai T., Mukai S., Hough J. H., 1987, A&A, 187, 689
- Kiselev, N., Velichko, S., Jockers, K., Rosenbush, V., and Kikuchi, S., Eds., Database of Comet Polarimetry. EAR-C-COMPIL-5-COMET-POLARIMETRY-V1.0. NASA Planetary Data System, 2006.
- Kiselev N.N., Rosenbush V.K., Afanasiev V.L., Blinov D.A., Kolesnikov S.V., Zaitsev S.V., 2012. Proceedings of the Asteroids, Comets, Meteors conference 2012. LPI contribution 1667, id.6102.
- Lamy P. L., Toth I., Weaver H. A., AHearn M. F., Jorda L., 2009, A&A, 508, 1045.
- Larson S., & Sekanina Z. 1984, AJ, 89, 571
- Levasseur-Regourd A.C., Hadamcik E., Renard J.B, 1996, A&A, 313, 327.
- Le Borgne J.F., Leroy J.L., Arnaud J., 1987, A&A, 187, 526
- Manset N., Bastien P., 2000, Icarus, 145, 203
- Medhi B. J., Maheswar G., Pandey J. C., Kumar T. S. and Sagar R., 2008, MNRAS, 388, 105
- Medhi B. J., Maheswar G., Brijesh K., Pandey J. C., Kumar T. S. and Sagar R., 2010, MNRAS, 378, 881
- Myers R. V., Icarus, 1985, 63, 206

- Nakano, S., 2011. Orbital Computations of Comet C/2009 P1 (Garradd). Oriental Astronomical Association. <a href="http://www.oaa.gr.jp/">http://www.oaa.gr.jp/</a> oaacs/nk.htm> (NK2109, NK1996, NK1953, NK1863).
- Pandey J. C, Medhi, Biman J., Sagar, R, Pandey A. K., 2009, MNRAS, 396, 100
- Paul D., Das H. S. and Sen A. K., 2012, BASI, 40, 113.
- Ramaprakash A. N., Gupta R., Sen A. K., Tandon S. N., 1998, A&AS 128, 369
- Rautela B. S., Joshi G. C. and Pandey J. C., 2004, BASI, 32, 159
- Renard J.-B., Hadamcik E. and Levasseur-Regourd, A.-C., A&A, 1996, 316, 263
- Schmidt G. D., Elston R., and Lupie O. 1992. ApJ, 104, 1564.
- Scarrott S. M., Warren-Smith R. F., Pallister W. S., Axon D. J. and Bingham R. G., 1983, MNRAS, 204, 1163
- Sen A. K. and Tandon S. N., 1994, Proc. SPIE Vol. 2198, p. 264-273, Instrumentation in Astronomy VIII, David L. Crawford; Eric R. Craine; Eds.
- Tanigawa M., Taniguchi T., Terao M., Fukui J., Ueda R., Sakamoto H., 2012, Proceedings of the Asteroids, Comets, Meteors conference 2012. LPI contribution 1667, id.6075.
- Turnshek D.A., Bohlin R.C., Williamson II R.L., Lupie O., Koornneef J., and Morgan D.H., 1990. Asytrophys. J. 99, 1243-1261.
- Villanueva G.L., Mumma M.J., DiSanti M.A., Bonev B.P., Paganini L., and Blake G.A., 2012. Icarus 220, 291-295 (2012)